Theoretical Studies on the Molecular Dependence of the Bond Dissociation after the Core Excitations. : $CH_3OCO(CH_2)_nCN$, n=0,1,2

Osamu TAKAHASHI, Masaki MITANI, Masanori JOYABU, Ko SAITO*, and Suehiro IWATA*

Department of Chemistry, Graduate School of Science, Hiroshima University, 1-3-1, Kagamiyama, Higashi-Hiroshima, 739-8526, JPN

Abstract

Approximate theoretical normal and resonant Auger spectra for a series of methyl cyanoesters were calculated. To study the reported molecular dependence of the fragmentation patterns after the core excitations, a new measure, bond dissociation factor, was introduced. The site-selectivity and the state-specificity for a series of methyl cyanoesters were qualitatively explained.

Key words: Site-specific bond dissociation, core excitation, Auger decay, bond dissociation factor, methyl cyanoester, molecular size dependency

[1]

[1]*Corresponding author. Tel.: +81-824-24-7405; Fax: +81-824-24-0726(K.Saito), Tel.: +81-3-4212-8050 fax:+81-3-4212-8121 (S.Iwata).

e-mail address: saito@sci.hiroshima-u.ac.jp(K.Saito), iwata@niad.ac.jp(S.Iwata)

1 Introduction

Photon stimulated desorption and dissociation (PSD) induced by core-level excitation of molecules using synchrotron radiation is one of the active fields both in surface science and in molecular physics. The site-specific bond scission following core excitation, in particular, has been drawn attention of many experimentalists [1–5]. The core electrons are localized on an atom, and the core excitation reflects the surrounding chemical environment of the atom. Thus, the excitation energy differs for the position of the atom, depending on where it is located in the molecule; with high resolution spectroscopy, a specific atom is selectively core-excited. The relaxation processes after the core excitation are also expected to be site-specific. The PSD is one of the most important relaxation processes after the core excitation. The reactions mostly proceed successively under three processes [6, 7]: (1)photoabsorption process, (2)energy relaxation processes, among which Auger decay process is dominant [8], and (3)bond dissociation (chemical reaction) process. By selecting an exciting energy in the photoabsorption, the initial states of reaction processes are chosen. A few reaction mechanisms are proposed [9–13]. Because the Auger decay process is the dominant energy relaxation process, it is expected that most of chemical reactions proceed after the Auger decay. To explore the reaction mechanisms experimentally, various multi-coincidence techniques were developed both for surface and gas phase experiments, such as photoelectron-photoion coincidence (PEPICO) and Auger electron-photoion coincidence (AEPICO).

Recently, Ibuki et al. studied the site-selective reactions for a series of methyl cyanoesters [5]. They examined the fragmentation patterns by exciting the N and O K shells of methyl cyanoformate (CH_3OCOCN) and methyl cyanoacetate (CH_3OCOCH_2CN). The fragmentation patterns were essentially identical in the N and O K-edge core excitations of methyl cyanoformate, whereas the state-specific and site-selective fragmentation patterns were observed for methyl cyanoacetate. A larger amount of N^+ ions was observed at N(1s) $\longrightarrow \pi^*$ excitation for methyl

cyanoacetate than at the other excitation energies. The difference of two molecules is a CH_2 between C=O and C≡N in methyl cyanoacetate, and therefore, they discussed the relationship between the site-selectivity and the molecular size.

Last decade theoretical studies on the core-excited states have made remarkable progress. Auger spectrum for atoms and small molecules was calculated with the large scale configuration interaction (CI) method [14] and with Green function method [15–17]. However, few investigations were reported for large molecules, which have different atomic sites for the same atomic species and thus may exhibit state-specific and site-selective relaxation processes [18]. The appropriate approximations applicable to calculating Auger transition energies and their transition probability are required. Furthermore, a tool to analyze the dissociation processes after the Auger decay in large molecules has to be developed, because it is almost prohibitive to calculate the potential energy surfaces for the dissociation channels of the molecules. Recently Nobusada and Tanaka performed the extensive CI calculations for the low-lying double cation states of a water molecule, H_2O^{2+}, and examined the potential energy surfaces for the analysis of the Auger dissociation process [19]. The similar calculations for our target molecules, such as methyl cyanoformate, are impossible to perform, and probably are meaningless, because of many possibilities of dissociation channels. A new approach is needed to get some insights of the selectivity of the reactions.

The purpose of the present study is to get some clues to understand the selectivity and non-selectivity observed by Ibuki et al. The target molecules are methyl cyanoformate(ester0), methyl cyanoacetate(ester1), and methyl cyanopropionate(ester2); three molecules differ by the number of CH_2 group between C=O and C≡N groups, 0, 1 and 2, respectively. The experimental study of Ibuki et al. has already been extended to methyl cyanopropionate [20]. To study the Auger spectra and the dissociation processes, we introduce a new factor, called bond dissociation factor (BDF), to get some measure of the easiness/difficulty of the dissociation of a particular bond after Auger decay, and discuss the reactivity of these molecules

after the core excitations.

2 Theoretical models

In the normal and resonant Auger transitions, the initial state with a core hole decays to the Auger final states having two valence holes. The Auger transition probability from the initial state to the final state with the holes at the vth and wth valence orbitals is given by

$$I_{vw} = 2\pi | < \Psi_f | \frac{1}{r_{12}} | \Psi_i > |^2, \tag{1}$$

where Ψ_i and Ψ_f are wave functions of the initial and final states, and r_{12} is the inter-electron distance, respectively. In the normal Auger transition, they are $(N-1)$ electrons wave functions, whereas these are N electrons wave functions in the case of the resonant Auger decay. The normal Auger transition intensity under a single electron configuration approximation is given [21, 22],

$$\begin{aligned}
{}^1I_{vv} &= 2\pi |(1sv|kv)|^2 \quad (v = w) \\
{}^1I_{vw} &= \pi |(1sv|kw) + (kv|1sw)|^2 \quad (v \neq w) \\
{}^3I_{vw} &= 3\pi |(1sv|kw) - (kv|1sw)|^2 \quad (v \neq w),
\end{aligned}$$

where a superscript of I indicates the spin multiplicity, and k and $1s$ indicate wave functions of Auger electron and core electron, respectively. Similar equations can be derived for the resonant Auger transition intensity as

$$\begin{aligned}
{}^2I_{vv} &= 2\pi |(1sv|kv)|^2 \quad (v = w) \\
{}^2I_{vw}(1) &= \pi |(1sv|kw) + (kv|1sw)|^2 \quad (v \neq w) \\
{}^2I_{vw}(2) &= 3\pi |(1sv|kw) - (kv|1sw)|^2 \quad (v \neq w).
\end{aligned}$$

It is noted that two kind of representations exist in the case of $v \neq w$. The Auger transition probability is expressed by two electron integrals involving the wavefunction of the Auger electron. For an atom and a diatomic molecule, the wavefunction

of the Auger electron could be solved numerically, but it is prohibitive for our target molecules. In this work, the Auger transition probability is simply approximated by the overlap between the core and valence molecular orbitals (MOs) by neglecting the term associated with the Auger electron. Because the core orbital is localized at an atom, the overlap between MOs may be estimated as the electron density of valence hole MOs on the core hole atom. For the overlap between MOs, Mulliken's population is adopted to calculate the Auger transition intensity.

In the present work, we avoid the so-called participator Auger electrons, main parts of which cannot be discerned from the resonantly enhanced photoelectron; Osborne et al [23] called it the Auger resonant Raman. Because of the different type of the matrix elements, the direct comparison of the intensity distribution is not possible.

Configuration Interaction (CI) expansion limited within the valence orbital space is used for the Auger final states. The nth final state wave function is written by a linear combination of two-hole spin-adapted configuration state functions (CSFs) $|\Psi_{vw}>$ for the normal Auger and by a linear combination of two-hole CSFs $|\Psi_{vw}>$ keeping an electron at the valence excited orbital for the resonant Auger as

$$|\Psi_n >= \sum_{v,w} |\Psi_{vw} > C_{vw,n} \tag{2}$$

where, $C_{vw,n}$ is the CI coefficient about each CSF and Ψ_{vw} is the two-hole CSF holed the vth and wth valence orbitals. Thus, the Auger transition probability to the nth state is given by

$$I_n = \sum_{vw} |C_{vw,n}|^2 \times I_{vw}. \tag{3}$$

The Auger electron kinetic energy KE for each of the Auger final state is obtained from the difference in total energies between the initial and final states, E and E_n, respectively.

$$KE = E_n - E \tag{4}$$

We are interested in the change in the bonding nature of a particular chemical bond via the photo-excitation of a core electron and the Auger decay. After the

Auger transition process, there are two holes at the valence orbitals. Thus the bond orders are expected to be changed from that in the initial state. The chemical bonds are weakened by removing electrons from the bonding orbitals. The change of the bond order upon the Auger transition could be used as a measure for the bond dissociation. The bond order is a concept extensively used in the empirical and semi-empirical MO (VB) theories. In the *ab initio* MO theory, the bond population can be used for the bond order. We define bond dissociation factor (BDF) between atom A and B defined as

$$D_n^{AB} = \sum_{vw} |C_{vw,n}|^2 \times I_{vw} \times \Delta P_{vw}^{AB}, \tag{5}$$

where, ΔP_{vw}^{AB} is difference of Mulliken's bond population [24] between the initial and nth Auger final states. We use the "bond dissociation factor (BDF)" D_n^{AB} as a measure of the change in the chemical bond between atom A and B, and we construct the theoretical AEPICO ion yield spectra. Furthermore, we may be able to define the sum over the states in Eq. (5) as a total bond dissociation factor (TBDF),

$$D^{AB} = \sum_n D_n^{AB}, \tag{6}$$

which may be used as a measure of easiness/difficulty of the dissociation of the chemical bond between atoms A and B. Experimentally, the fragment ions detected without coincidence correspond to the TBDF.

It is noted that BDF, which we defined, cannot distinguish the position of charge. For example, in the case of the normal Auger process, the following three types of fragmentation are possible,

$$\begin{aligned} (A--B)^+ &\longrightarrow A^{2+} + B \\ &\longrightarrow A^+ + B^+ \\ &\longrightarrow A + B^{2+}. \end{aligned}$$

It is expected that the possibility of production of a pair of single-charged ions is higher than that of a pair of the multi-charged ion and neutral fragment. And in

the case of the spectator Auger process, the following two types of fragmentation are possible,

$$\begin{aligned}(A--B) &\longrightarrow A^+ + B \\ &\longrightarrow A + B^+.\end{aligned}$$

These cannot be distinguished in our model. We assume that these two processes may happen equally.

3 Calculational Procedure

Geometry optimizations for ester0, ester1, and ester2 are performed using Gaussian 98 [25] at the HF/6-31(d,p) level of approximation. There are many conformations for each molecule. Here the most stable conformation (all trans conformer) is examined. They are shown in Fig. 1.

For the Auger transition probability calculations, Dunning's correlation consistent basis sets [26] (cc-pVDZ) is used. For the normal Auger decay, the ground state MOs without the core hole are used, whereas, for the resonant Auger decay, the core-hole state MOs are determined by the electron-hole potential (EHP) method by Iwata and Morokuma [27] to include the core-hole relaxation.

Limited spin-symmetry adapted CI calculations within the two-hole valence space are performed. For the normal Auger transition, the initial wave function is the doublet state, and thus the spin multiplicity of the Auger final state is both the singlet and triplet states. On the other hand, for the resonant Auger transition, the initial wave function is the singlet state. The possible spin multiplicity of the Auger final state is the doublet state only. Because our target systems do not have any heavy atoms, the spin-forbidden process is neglected. There are two kinds of the resonant Auger transitions, one is the participator Auger, in which the excited electron participate in Auger process, and the other is the spectator Auger, in which the excited electron stays at the orbital [8]. For the mechanism of the site-specific

and state-specific bond dissociation, the spectator Auger process is more important, because both valence orbitals and an excited orbital are contributed. Thus the participator Auger is neglected in our study. The theoretical Auger line spectrum is convoluted with Gaussian of 5.0 eV FWHM to represent the real spectrum, because the present target molecules are so large that there are many Auger final states. The bond dissociation factor and total bond dissociation factor are evaluated and their spectrum is also convoluted with Gaussian of 5.0 eV FWHM.

4 Results and discussion

4.1 Auger decay spectra

The calculated resonant and normal Auger spectra in Eq. (3) of ester0 for N(1s) $\longrightarrow \pi(\mathrm{C{=}O})^*$, N(1s) $\longrightarrow \pi(\mathrm{C{\equiv}N})^*$ excitation, and N(1s) ionization are shown in Fig. 2. The stick spectrum is also given at the bottom of the figure. As are seen from the spectra, there are so many final states possible, even without counting the shake-up type final states. For example, in the normal Auger transitions of ester0, there are 256 final states. Thus, the detailed assignment of the final state of each transition is almost meaningless. All of the calculated Auger spectra in our present study are grouped in three parts. The spectra shown in Fig. 2 are typical of them. The highest peak around 390 eV is assigned to the states having two outer-valence holes. The final states of the second peak near 365 eV have the holes in the outer- and inner-valence orbitals. The last group of the final states, which peak near 345 eV, have both holes in inner-valence orbitals. The state density is more important rather than each Auger transition intensity calculated from Eq. (3). As seen in the bottom of the figure the state density differs by the energy region; thus the spectrum pattern in Fig. 2 is determined.

Fig. 3 compares the calculated normal (a) and resonant (b) Auger spectra of three molecules at the N K-edge excitations. The spectra resemble one another

in the pattern, indicating that the character of MOs, which have a large overlap with the N(1s) core orbital, almost similar to each other. The spectra of ester2 have less structures than the other two molecules. Too many final states blur the spectrum in this large molecule. More important difference is found in the relative intensity among three groups of the peaks in the resonant Auger spectra of N(1s) $\longrightarrow \pi(\mathrm{C}{\equiv}\mathrm{N})^*$ in Fig. 3(b). The first peak in ester2 becomes more dominant than in ester0 and ester1. This difference suggests that as the molecular size becomes large, both valence and unoccupied $\pi(\mathrm{C}{\equiv}\mathrm{N})^*$ orbitals are relatively more localized.

4.2 Bond dissociation

Figure 4 shows the excitation dependence of the bond dissociation factor (BDF) spectrum of the C≡N triple bond in ester0 for the normal and resonant Auger transitions. The BDF is defined by Eq. (5). The spectra should correspond to the AEPICO ion yield spectrum of N^+ ions in the experiment. However, AEPICO experiments for our target molecules have not been studied yet. In the figures the calculated Auger spectrum is also shown in a thin solid line. The comparison of the BDF spectra of four excitations is suggestive. At the excitations to the π^*(C=O) and π^*(C≡N) the calculated Auger and BDF spectra are similar to each other. The similarity in the Auger and BDF spectra of two excitations is reasonable. In ester0 C=O and C≡N are conjugated, and in reality two π^* orbitals have more or less both characters. The relative intensity of the Auger transitions and BDF reflect the local nature around the N atom in the molecular orbitals involved, and therefore, the excitation to the orbital, whose main character is π^*(C=O) with a minor contribution from π^*(C≡N), yields an almost identical spectrum with the excitation to the orbital whose main character is π^*(C≡N). In these excitations, both the Auger and BDF spectra are similar to each other, suggesting that these excitations are important to the C≡N bond scission.

Contrary to the excitations to the π^* orbitals, the Auger and BDF spectra of

the $\sigma^*(CH_3)$ excitation and the normal Auger process are very different. Both BDF spectra show rich structures below 380 eV, and the intensity of the second peak is larger than that of the first one. Those peaks are the transitions to the states having the holes in the outer-valence and inner-valence orbitals. The $\sigma^*(CH_3)$ orbital is located at an opposite side from the N atom, which is core-excited. The core orbital is less overlapped with the orbitals related to the strength of the C≡N bond. The difference in two spectra suggests that the MOs contributing to the Auger intensity is not always same with the MOs contributing to the nearest chemical bond of the excited atom.

Now, we examine the molecular size dependence in the BDF spectra at the C≡N triple bond for N K-edge. Fig. 5 compares the BDF spectra for (a) normal Auger process and (b) the excitation to the π^*(C≡N) of ester0, ester1 and ester2. These spectra resemble each other, indicating that characters of MOs, in terms of the overlap with the N(1s) core orbital, are almost same. Some of shoulders disappear in the spectra of ester2, because the number of states become larger than ester0 and ester1, and the density of state becomes large. For ester1 and ester2, in particular at the π^*(C≡N) excitation, the relative intensity of the band around 385 eV increases substantially, which implies that the CN bond break is more strongly correlated to the two outer-valence hole states.

Finally, we discuss the total bond dissociation factors (TBDF, D^{AB}), which could correspond to the data experimentally obtained by Ibuki et al. [5]. Figs. 6 and 7 compare the molecular dependences of ester0, ester1 and ester2. Fig. 6 examines the bond dependence for the normal Auger transition at the N and O(carbonyl) K-edges. To see the bond dependency, TBDF is normalized to 1 for the C≡N bond. At the N K-edge excitation, TBDF for the C≡N bond is dominant in all of three molecules. It is more so for ester2, which we may call molecular size effect. Note that the bond break at the C≡N produces the N^+ ion. The calculated TBDF qualitatively measures the molecular size effect reported by Ibuki et al. [5] It could be noticed that D^{AB} for the neighboring bond C-CN is the smallest among the bonds. Except

for this bond, D^{AB} becomes smaller for more distant bonds from the excited atom N. At the O(carbonyl) K-edge excitation shown in Fig. 6(b), $D^{C\equiv N}$ for the C≡N bond is as large as that for the C=O bond. The molecular and bond dependences are less apparent than at the N K-edge excitation, which is also consistent with the reported findings.

In Fig. 7, the excitation dependences for three molecules at near N and O(carbonyl) K-edges are compared. The TBDF in this figure is normalized to the normal Auger process. A slight molecular size effect is found in the excitation dependence. In ester0, $D^{C\equiv N}$ is almost 1, irrelevant of the excitations. On the other hand, in ester1 and ester2, $D^{C\equiv N}$ is larger at the π^*(C≡N) excitation, and smaller at the π^*(C=O) excitation than at the normal Auger process. At the near O K-edge excitations of carbonyl, all of the resonant excitations examined enhance the TBDF, except for the $\sigma^*(CH_3)$ excitation in ester0. With this exception the TBDF of ester0 is less excitation-dependent than in ester1 and ester2.

From the above discussion, using the TBDF, we might be able to qualitatively explain the difference of reactivity between ester0 and ester1. In the experimental report by Ibuki et al. [5], the site-specificity was not observed for ester0, whereas it was observed for ester1. If a CH_2 group is inserted, the valence molecular orbitals turned to be localized on each functional group. There is another difference in ester0 from in ester1 and ester2. In ester0, the π orbitals of C=O and C≡N are conjugated. On the other hand, they are not in ester1 and ester2. This difference changes the character of the excited orbitals π^*(CO) and π^*(CN). More systematic studies, both experimentally and theoretically are required to clarify the unique chemical reactions of polyatomic molecules after the core excitation.

In our studies, the discussion is only based on the electronic structure of chemical bonds in the molecules. As mentioned in Introduction, the photodissociation processes after the core excitations are various competing processes and not a single step dissociation. To explore the processes, we are aware of the limitation of the present treatment. We have to study the rates of the competing processes. For

instance, in some core excitations, it is now known that the dissociation process proceeds before the Auger decay.

Our study is an attempt; more improved treatments are required in future works. First, MOs using the normal Auger decay are those of the ground state without the core hole. By the core hole relaxation, Auger spectra will be changed. Second, molecular geometries are fixed at the equilibrium geometry. The core hole state has some life time, which is very short. While there are the core hole states, something geometry relaxation will be expected. Third, it is possible to define BDF by another quantity, for example, BDF can also be defined to the gradient of the potential surface. Forth, charge distribution in molecule after Auger decay should be considered. We have to overcome these difficulties to make clear the mechanism for site-selective reactions.

5 Acknowledgement

The study is supported by a Grant-in-Aid on Research for the Future "Photoscience" (JSPS-RFTF-98P01202) from Japan Society for the Promotion of Science. The authors thank to Prof. Tanaka, Prof. Hiraya, Prof. Sekitani and Dr. Wada of the research group for helpful discussion. The authors thank the Institute for Non-linear Science and Applied Mathematics at Hiroshima University, for the use of COMPAQ Personal Workstation 433au.

References

[1] W.Eberhardt, T.K.Sham, R.Carr, S.Krummacher, M.Strongin, S.L.Weng, D.Wesner, Phys. Rev. Lett. 40 (1983) 1038.

[2] D.M.Hanson, Adv. Chem. Phys. 77 (1990) 1.

[3] S.Nagaoka, K.Mase, I.Koyano, Trends Chem. Phys. 6 (1997) 1.

[4] T.Sekitani, E.Ikenaga, K.Fujii, K.Mase, N.Ueno, K.Tanaka, J. Elec. Spectro. Related Phenomena 101-103 (1999) 135.

[5] T.Ibuki, K.Okada, K.Saito, T.Gejo, J. Elec. Spectro. Related Phenomena 107 (2000) 39.

[6] T.E.Madey, D.E.Ramaker, R.Stockbauer, Ann. Rev. Phys. Chem. 35 (1984) 215.

[7] V.Rehn, R.A.Rosenberg, in: R.Z.Bachrach (Ed.), Synchrotron Radiation Research –Advances in Surface and Interface Science, Vol. 1, Plenum Press, 1984, p. 327.

[8] T.A.Carlson, Photoelectron and Auger Spectroscopy, Plenum Press, 1975, p. 279.

[9] D.Menzel, R.Gomer, J. Chem. Phys. 41 (1964) 3311.

[10] P.A.Redhead, Can. J. Phys. 42 (1964) 886.

[11] P.Antoniewicz, Phys. Rev. B 21 (1980) 3811.

[12] D.E.Ramaker, C.T.White, J.S.Murday, J. Vac. Sci. Technol. 18 (1981) 748.

[13] D.E.Ramaker, C.T.White, J.S.Murday, Phys. Lett. A 89 (1982) 211.

[14] E.Kukk, J.D.Bozek, W.-T.Cheng, R.F.Fink, A.A.Wills, N.Berrah, J. Chem. Phys. 111 (1999) 9642.

[15] L.S.Cederbaum, P.Campos, F.Tarantelli, A.Sgamellotti, J. Chem. Phys. 95 (1991) 6634.

[16] D.Minelli, F.Tarantelli, A.Sgamellotti, L.S.Cederbaum, J. Chem. Phys. 99 (1993) 6688.

[17] K.Zähringer, H.-D.Meyer, L.S.Cederbaum, F.Tarantelli, A.Sgamellotti, Chem. Phys. Lett. 206 (1993) 247.

[18] F.Tarantelli, A.Sgamellotti, L.S.Cederbaum, J.Schirmer, J. Chem. Phys. 86 (1987) 2201.

[19] K.Nobusada, K.Tanaka, J. Chem. Phys. 112 (2000) 7437.

[20] K.Okada, et al., to be published.

[21] V.Carravetta, H.Ågren, Phys. Rev. A 35 (1987) 1022.

[22] E.O.Sako, Y.Kanameda, E.Ikenaga, M.Mitani, O.Takahashi, K.Saito, S.Iwata, S.Wada, T.Sekitani, K.Tanaka, J. Electro. Spec. Related Phenomena 114-116 (2001) 591.

[23] S. J. Osborne, A. Ausmees, S. Svensson, A. Kivimäki, O. P. Sairanen, A. N. de Brito, H. Aksela, S. Aksela, J. Chem. Phys. 102 (1995) 7317.

[24] R.S.Mulliken, J. Chem. Phys. 23 (1955) 1833.

[25] M. J. Frisch, G. W. Trucks, H. B. Schlegel, G. E. Scuseria, M. A. Robb, J. R. Cheeseman, V. G. Zakrzewski, J. A. Montgomery, J. R. E. Stratmann, J. C. Burant, S. Dapprich, J. M. Millam, A. D. Daniels, K. N. Kudin, M. C. Strain, O. Farkas, J. Tomasi, V. Barone, M. Cossi, R. Cammi, B. Mennucci, C. Pomelli, C. Adamo, S. Clifford, J. Ochterski, G. A. Petersson, P. Y. Ayala, Q. Cui, K. Morokuma, D. K. Malick, A. D. Rabuck, K. Raghavachari, J. B. Foresman, J. Cioslowski, J. V. Ortiz, B. B. Stefanov, G. Liu, A. Liashenko, P. Piskorz,

I. Komaromi, R. Gomperts, R. L. Martin, D. J. Fox, T. Keith, M. A. Al-Laham, C. Y. Peng, A. Nanayakkara, C. Gonzalez, M. Challacombe, P. M. W. Gill, B. Johnson, W. Chen, M. W. Wang., J. L. Andres, C. Gonzalez, . Head-Gordon, E. S. Replogle, J. A. Pople, Gaussian 98, revision a.4.

[26] J. T.H.Dunning, J. Chem. Phys. 90 (1989) 1007.

[27] K.Morokuma, S.Iwata, Chem. Phys. Lett. 16 (1972) 192.

Figure captions.

- Fig.1 Optimized geometric structures of the target molecules. (a)Methyl cyanoformate (ester0). (b)Methyl cyanoacetate (ester1). (c)Methyl cyanopropionate (ester2).

- Fig.2 Calculated Auger spectra of methyl cyanoformate (ester0) excited at the near N K-edge. Theoretical curves are obtained by Gaussian convolution of the calculated Auger transition probability with FWHM 5.0 eV. The stick spectra are also in the figures. (a)Resonant Auger spectrum for the N(1s) $\longrightarrow$ π(C=O)* excitation. (b)Resonant Auger spectrum for the N(1s) $\longrightarrow$ π(C$\equiv$N)* excitation. (c)Normal Auger spectrum.

- Fig.3 Comparison of the calculated Auger spectra of ester0, ester1, and ester2 excited at the near N K edge. (a)Normal Auger spectrum. (b)Resonant Auger spectrum for the N(1s) $\longrightarrow$ π(C$\equiv$N)* excitation.

- Fig.4 Excitation dependence of the calculated Auger (solid line) and dissociation factor (solid line with square symbol) spectra of methyl cyanoformate (ester0) at the near N K-edge. Theoretical curves are obtained by Gaussian convolution of the calculated Auger transition probability with FWHM 5.0 eV. (a)Excitation at N(1s) $\longrightarrow$ π(C=O)*. (b)Excitation at N(1s) $\longrightarrow$ σ(CH$_3$)*. (c)Excitation at N(1s) $\longrightarrow$ π(C$\equiv$N)*. (d)Normal Auger transitions.

- Fig.5 Comparison of the calculated bond dissociation factor (BDF) spectra of the C$\equiv$N triple bond in ester0, ester1, and ester2, excited at the near N K-edge. (a)Normal Auger transitions. (b)Resonant Auger transitions for the N(1s) $\longrightarrow$ π(CN)* excitation.

- Fig.6 Relative total bond dissociation factors for some of the chemical bonds in the the normal Auger transitions defined by Eq. (6). The values are normalized to 1 for the C$\equiv$N bond. (a)At the N K-edge. (b)At the O K-edge.

- Fig.7 Excitation dependence of the relative total bond dissociation factors. (a) At the N K-edge. (b) At the O K-edge. The values are normalized to 1 for the normal Auger.

CH_3OCOCN (ester0)

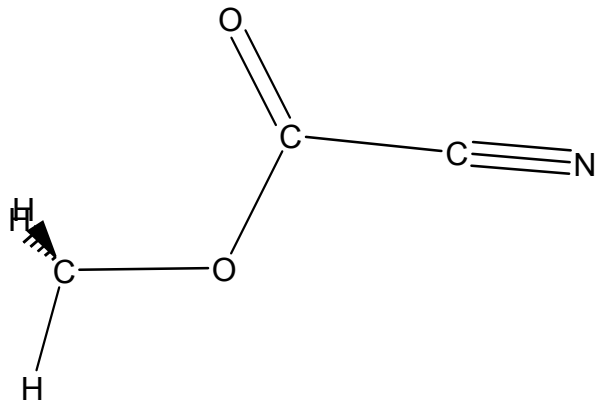

CH_3OCOCH_2CN (ester1)

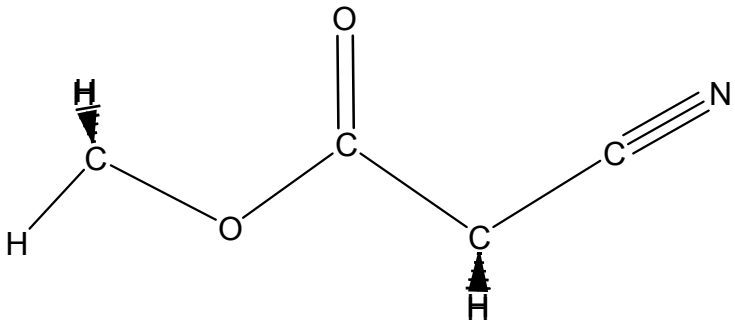

$CH_3OCOCH_2CH_2CN$ (ester2)

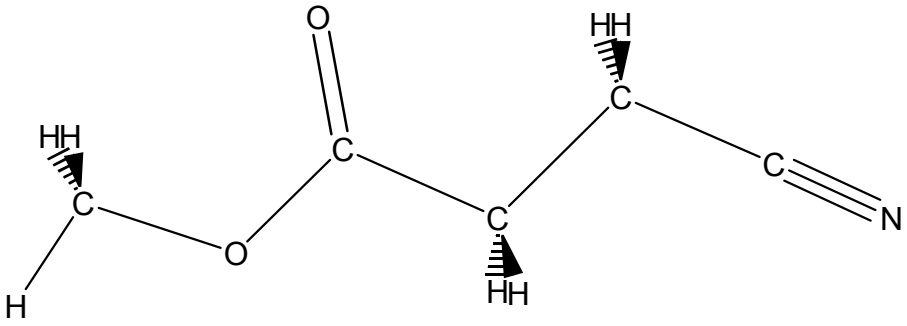

fig.1 Takahashi et al.

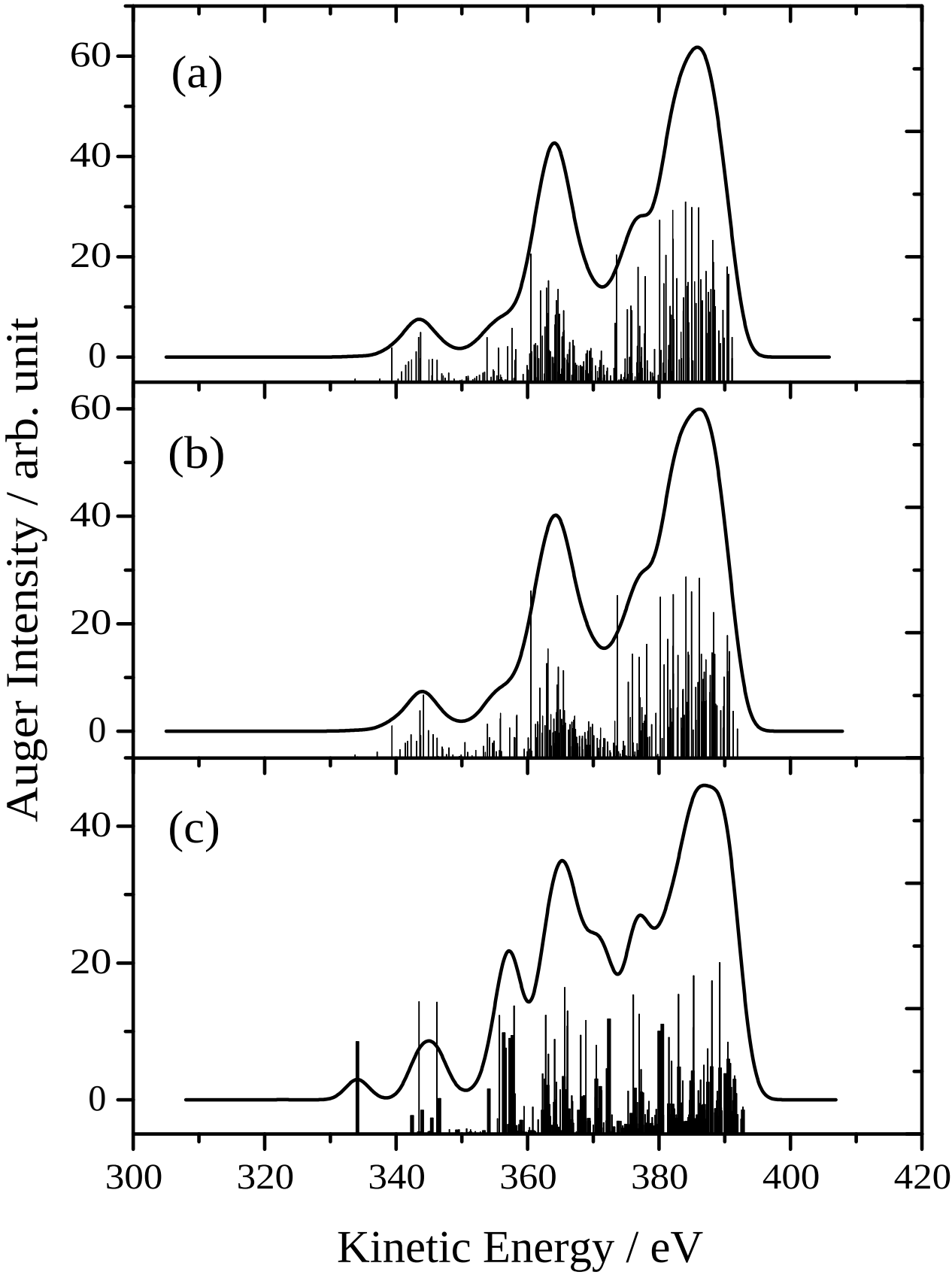

Fig.2 Takahashi et al.

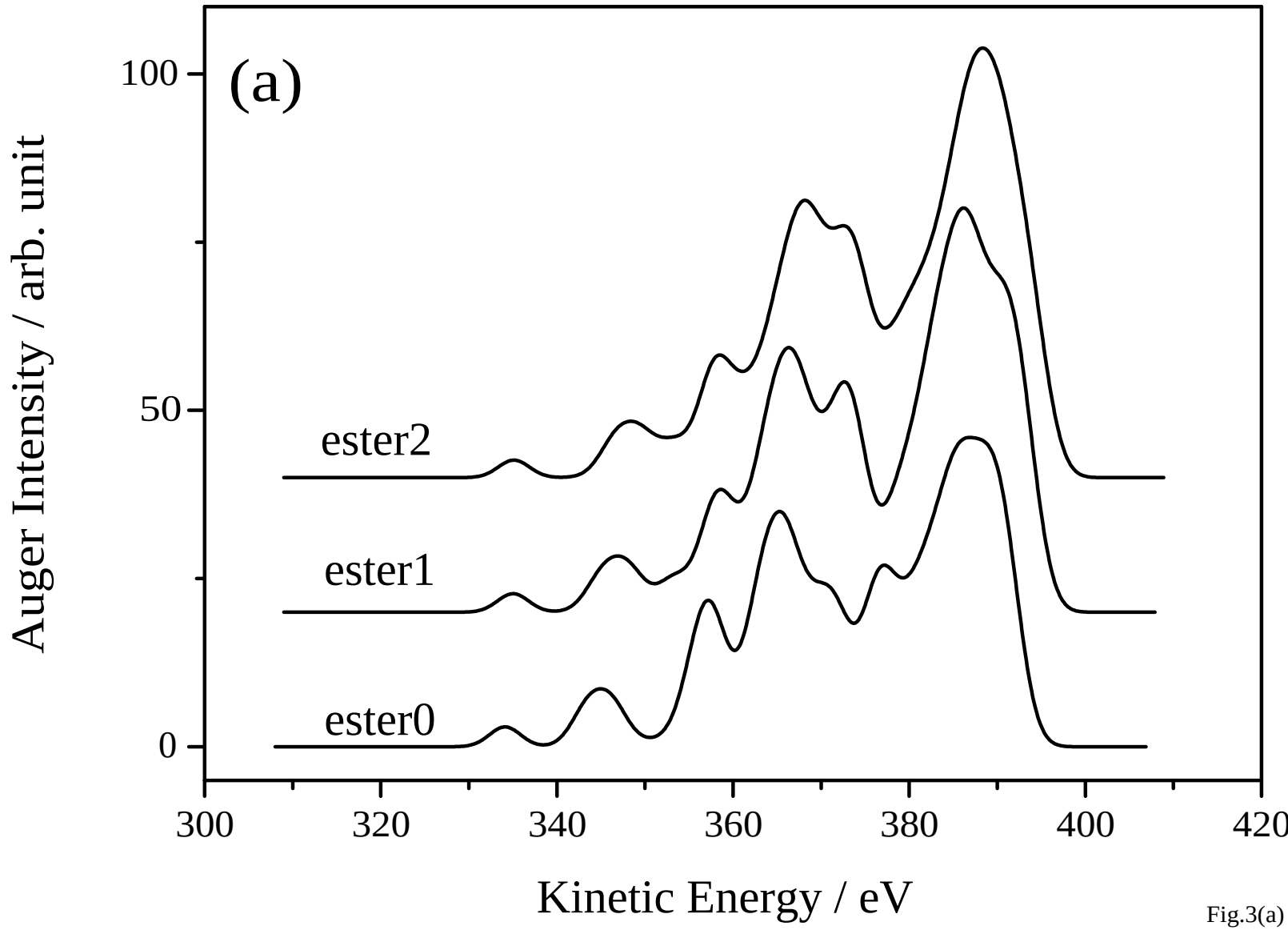

Fig.3(a) Takahashi et al.

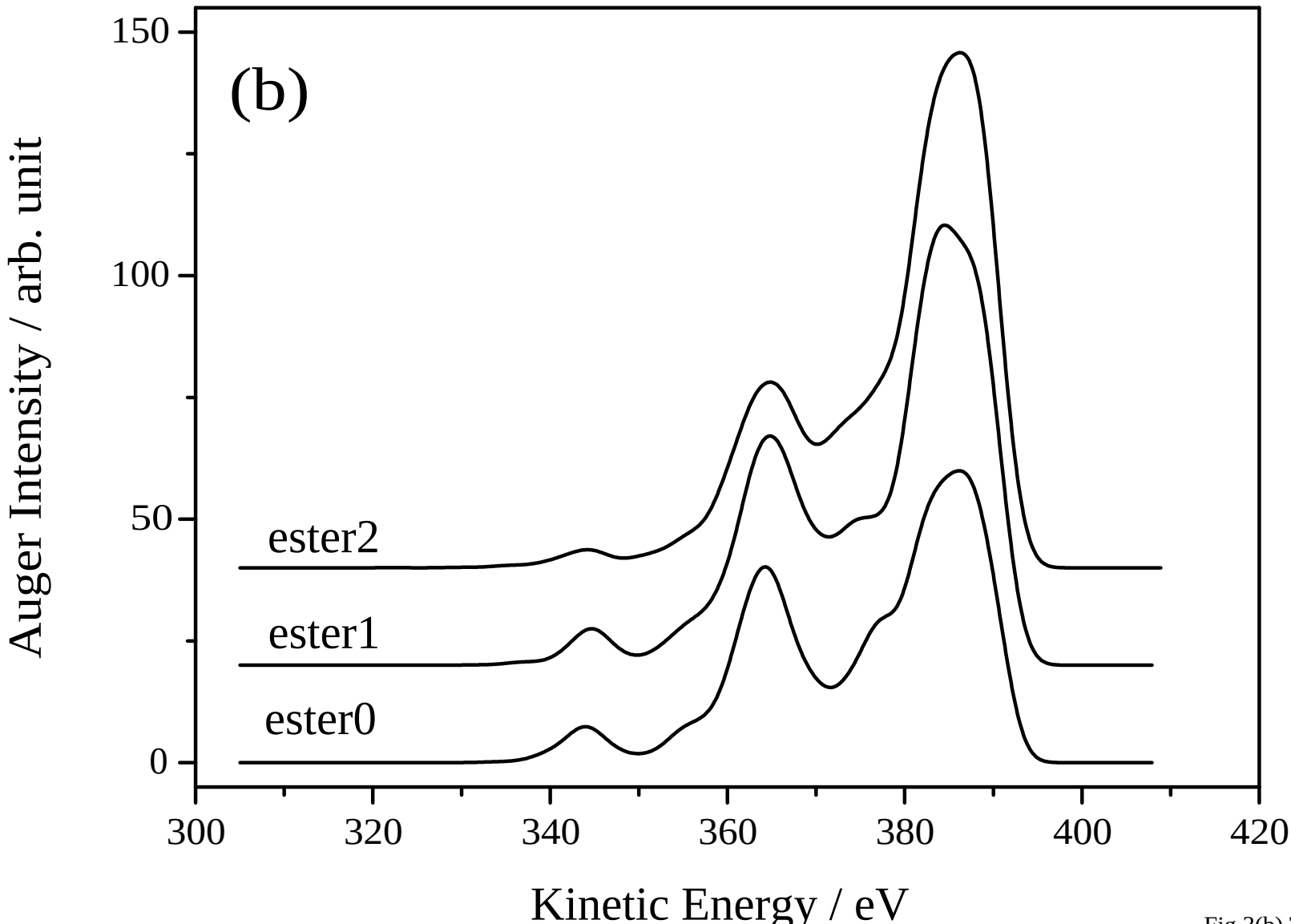

Fig.3(b) Takahashi et al.

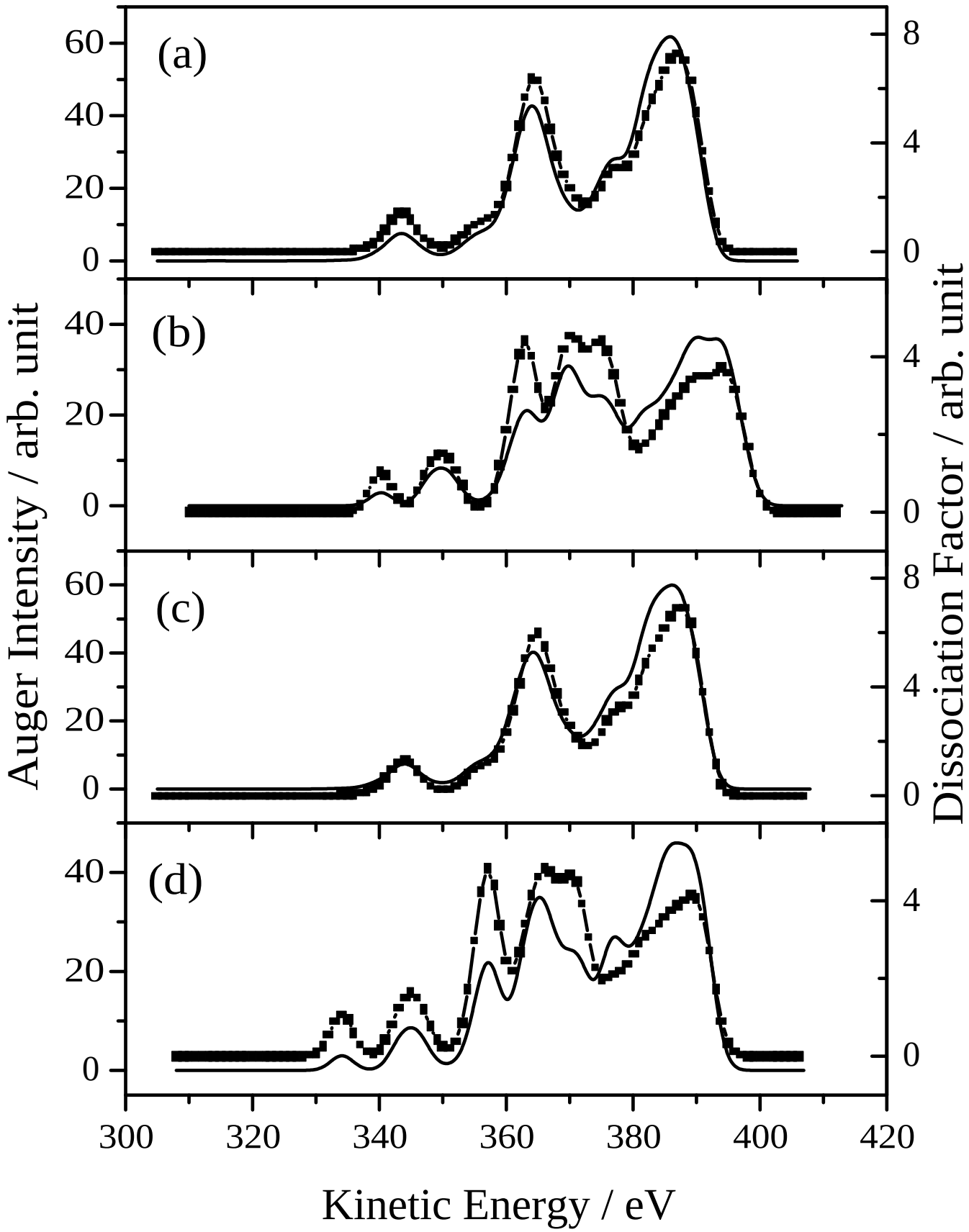

Fig.4 Takahashi et al.

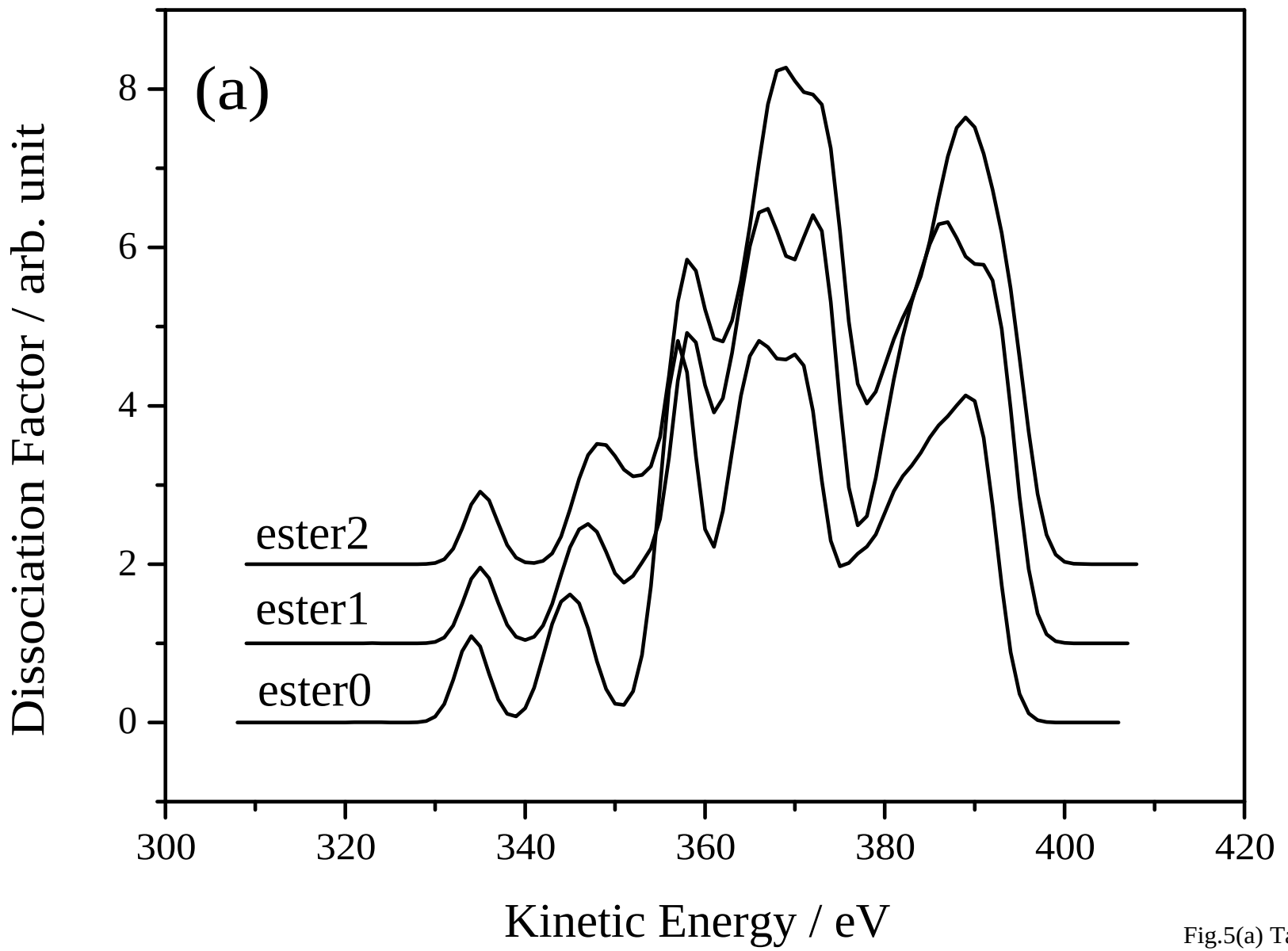

Fig.5(a) Takahashi et al.

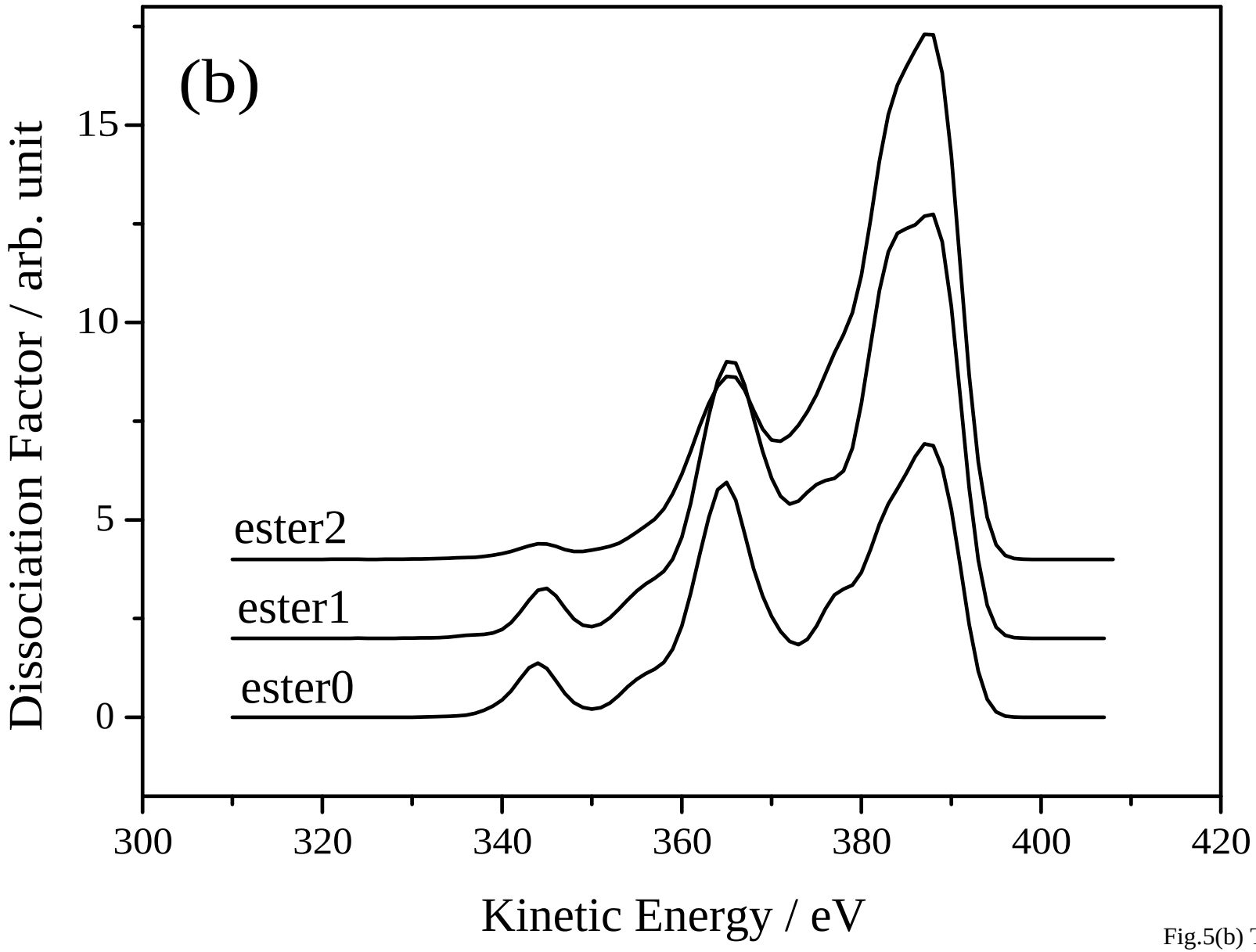

Fig.5(b) Takahashi et al.

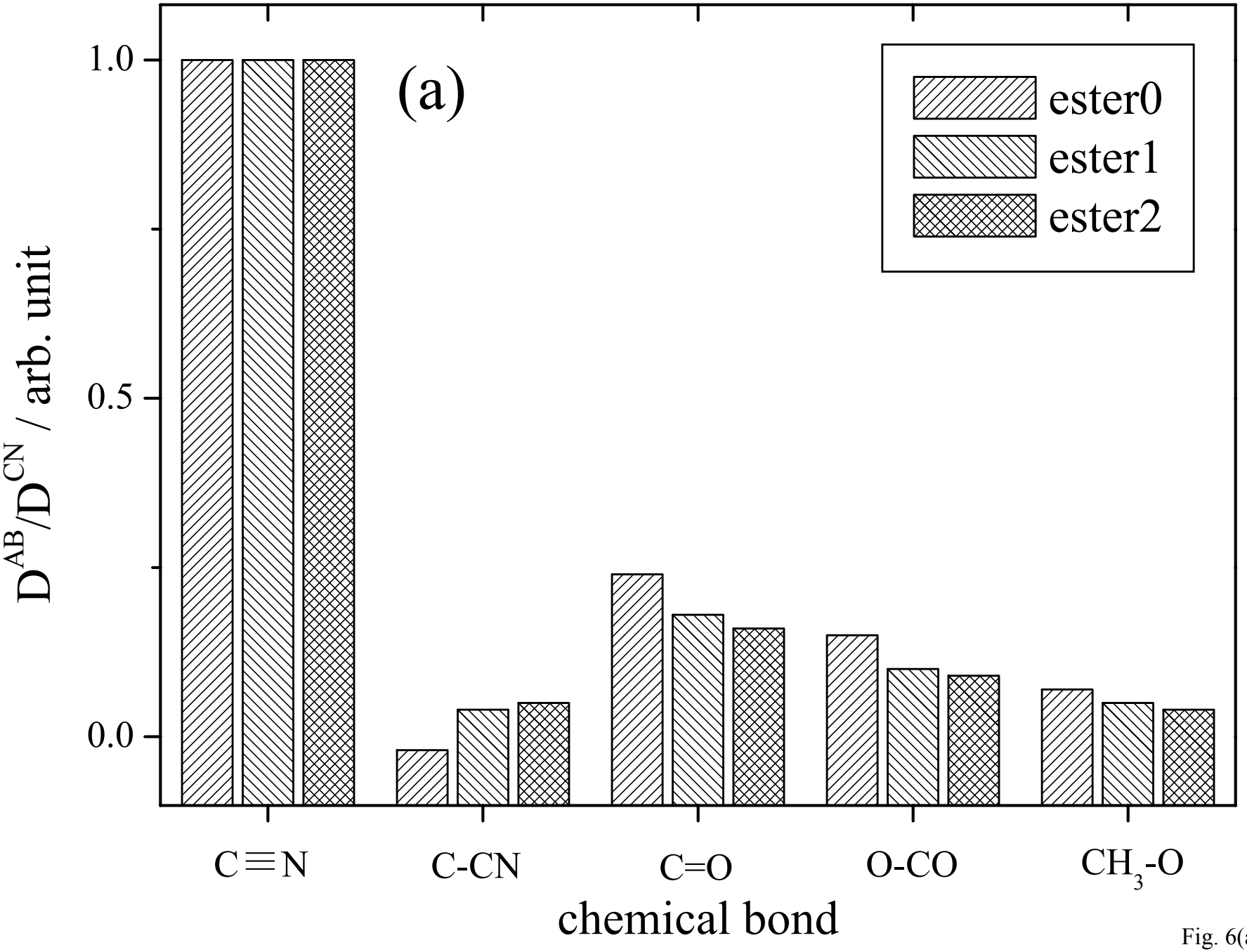

Fig. 6(a) Takahashi et al.

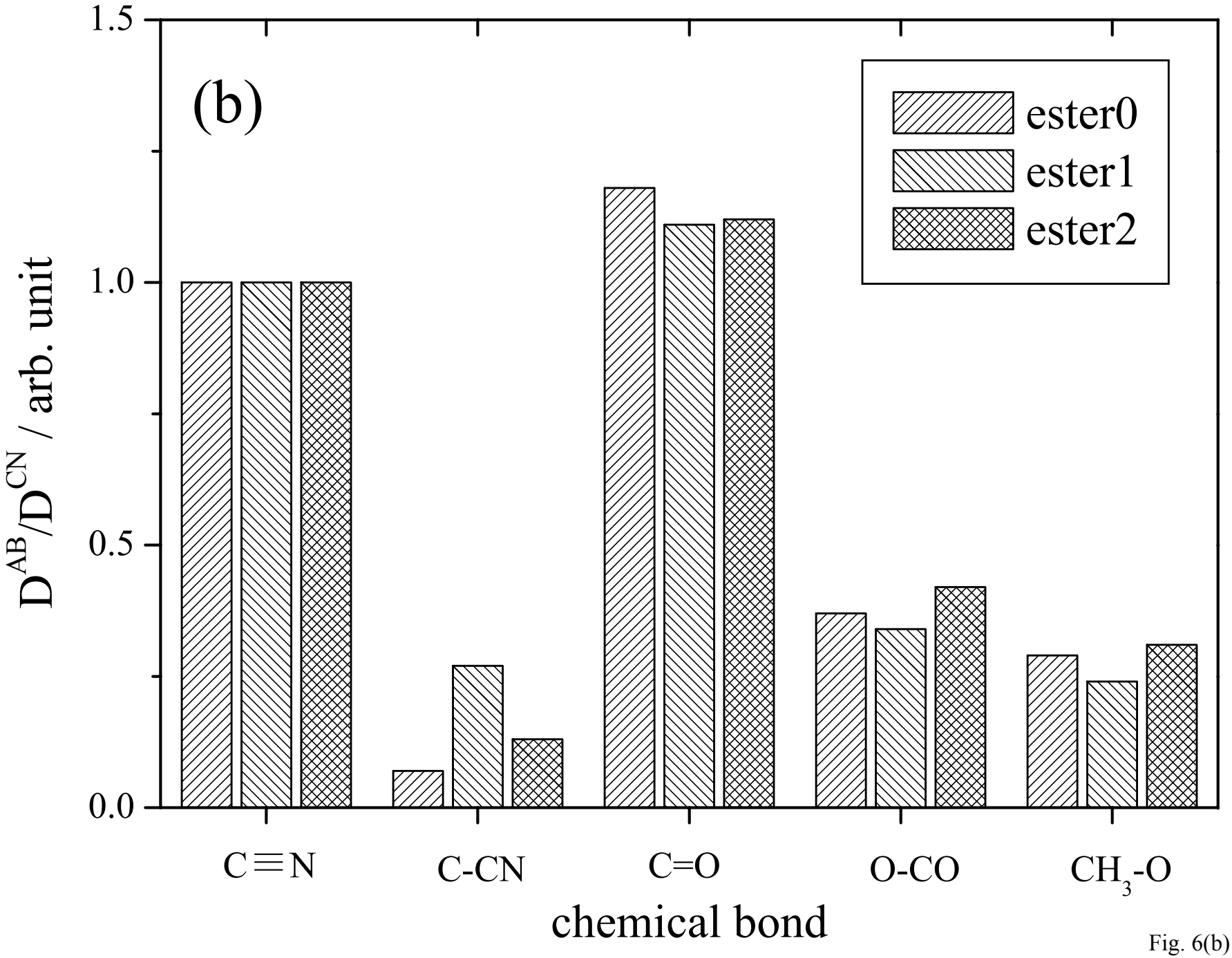

Fig. 6(b) Takahashi et al.

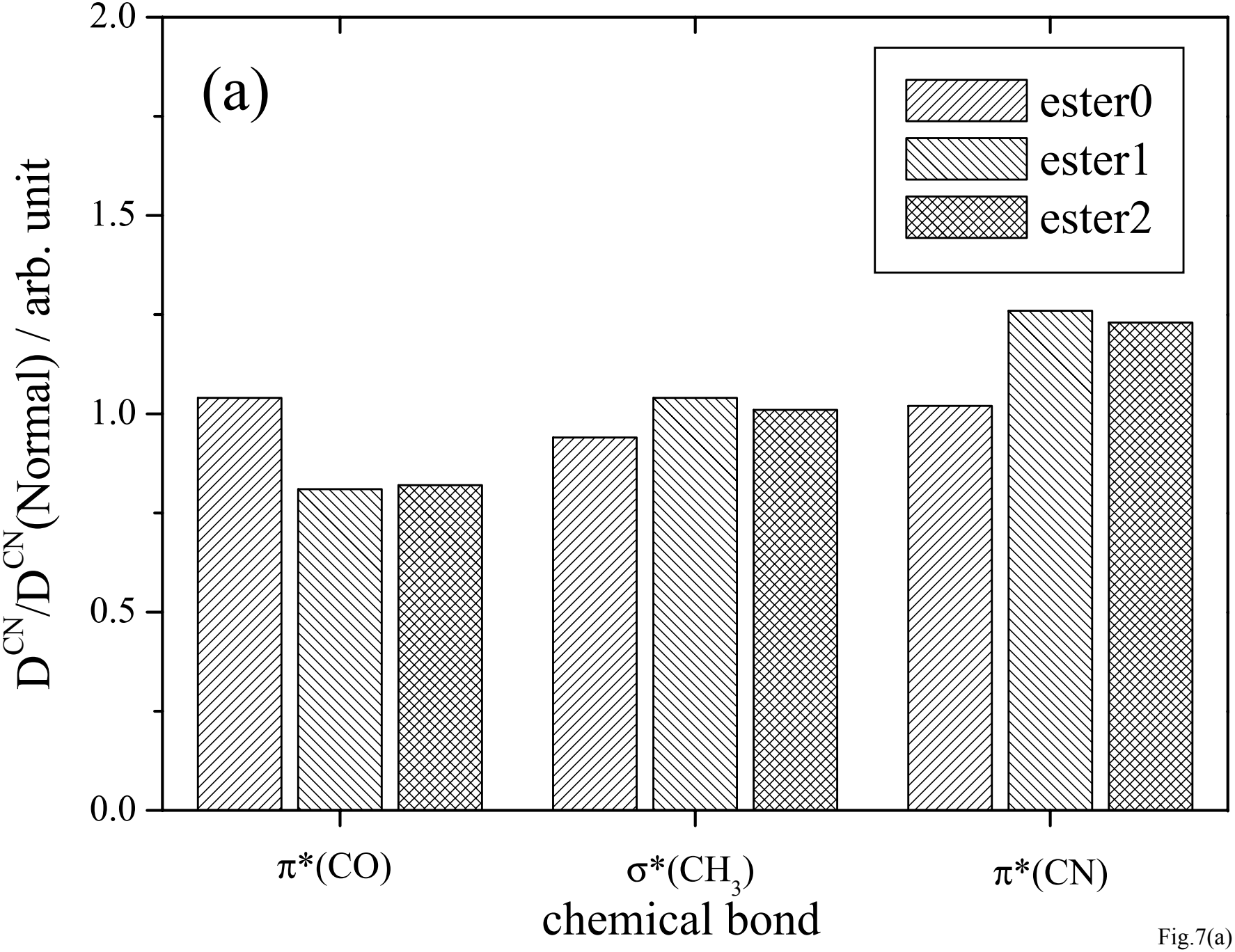

Fig.7(a) Takahashi et al.

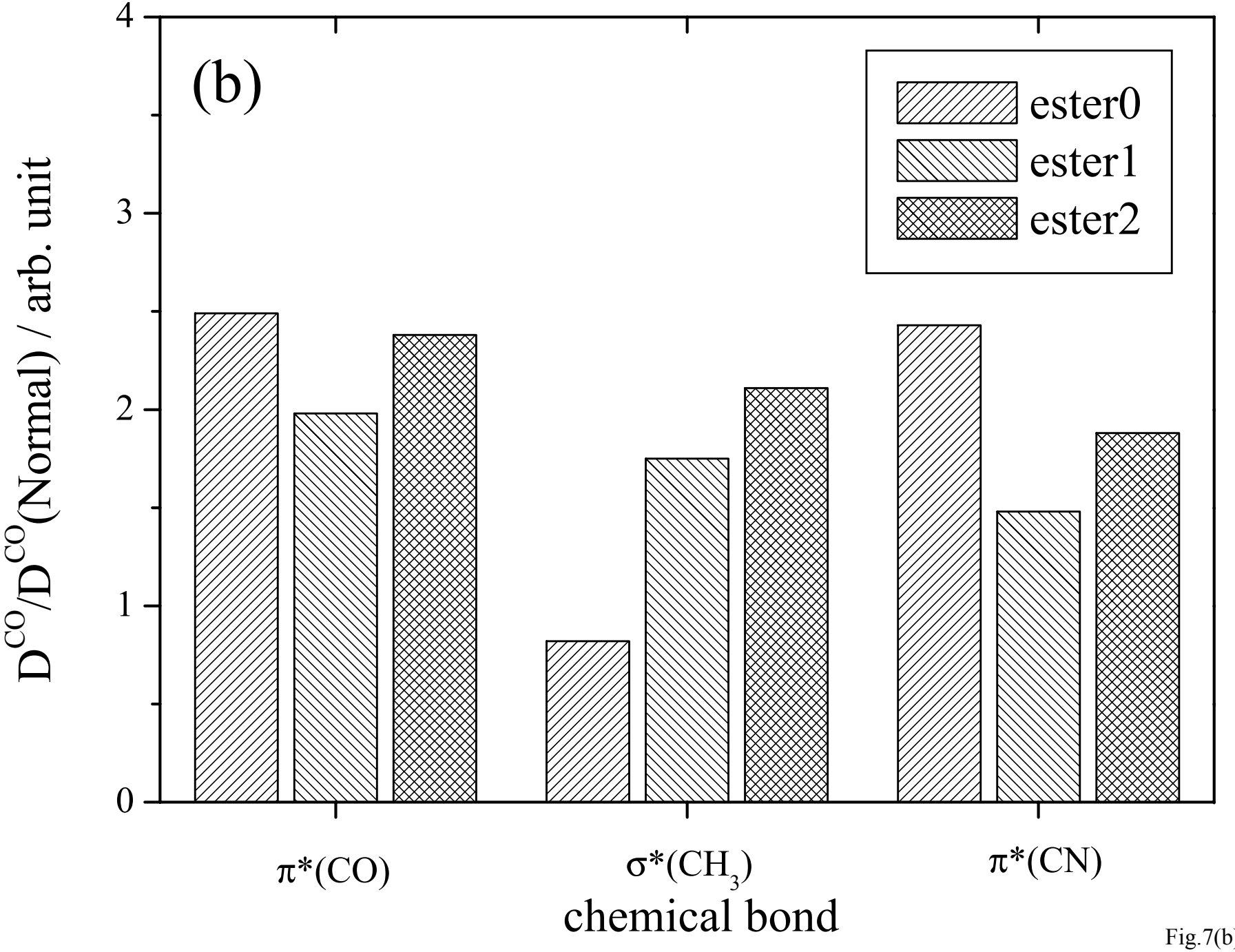

Fig.7(b) Takahashi et al.